Proceedings of the ASME 2023
42nd International Conference on Ocean, Offshore Arctic Engineering
OMAE2023
June 11-16, 2023, Melbourne, Australia

OMAE2023-103432

COMPARISON BETWEEN EXPERIMENTS AND SIMULATIONS FOR A SHIP MANEUVERING IN WAVES

Krishnavelu R[1], Visharad Borsutkar[1], Abhilash Somayajula[1]

[1]Department of Ocean Engineering, Indian Institute of Technology Madras, Chennai, Tamilnadu, India

ABSTRACT

The current regulations of the International Maritime Organization (IMO) aims to increase the reduction of carbon dioxide (CO_2) emissions from shipping by providing mandates to improve the Energy Efficiency Design Index (EEDI) of new ships. This has prompted newer vessels to be equipped with low-powered engines as compared to the previous vessels of similar size. However, the low power may potentially cause some vessels to be ill-equipped to maneuver effectively in the presence of waves. Although, traditionally turning characteristics of a vessel is considered in calm waters, in light of the new regulations it is important to consider course-changing ability in waves during the design process. This study aims to compare the maneuvering simulations and experiments of a scaled KRISO container ship (KCS) in calm water and in regular waves. The MMG standard method was developed by the Maneuvering Mathematical Group (MMG) which was organized by the Japan Society of Naval Architects and Ocean Engineers. This model is used to simulate the motions of the vessel in still water. A potential flow theory-based MDLHydroD software is used for calculating second-order wave drift forces and these drift forces are added to the MMG model. The simulations are compared with free-running model tests in both calm water conditions and in regular waves.

Keywords: Maneuvering, MMG model, Hydrodynamic, IMO, EEDI, (CO_2), KCS, Second-order wave drift force, Added resistance, Numerical simulation, Regular waves.

NOMENCLATURE

A_R	Profile area of a movable part of mariner rudder
a_H	Rudder force increase factor
B	Ship breadth
C_b	Block coefficient
D_p	Propeller diameter
d_{em}	ship draft (d)
F_N	Rudder normal force
F_n	Froude number based on ship length
H_R	Rudder spank length
I_{zG}	Moment of inertia of ship around center of gravity
J_p	Propeller advance ship
J_z	Added moment of inertia
K_T	Propeller thrust open water characteristic
k_2	Coefficient representing K_T
k_1	Coefficient representing K_T
k_0	Coefficient representing K_T
L_{PP}	Ship length between perpendiculars
ℓ_R	Effective longitudinal coordinate of rudder position in formula of β_R
M_z	Yaw moment acting on the ship around the center of gravity
m	Ship's mass
m_x	Added mass in x direction
m_y	Added mass in y direction
np	Propeller revolution
o	Ship fixed coordinate system taking the origin at midship. x,y,z axis
o_0	Space fixed coordinate system, x_0, y_0, z_0 axis
$X_0^{'}$	Ship resistance coefficient in straight moving
r	Yaw rate
T	Propeller Thrust
t	Time
t_p	Thrust deduction factor
t_R	Steering resistance deduction factor
U	Resultant speed = $\sqrt{u^2 + v^2}$
U_0	Desired ship speed
U_R	Resultant inflow velocity to rudder
u	surge velocity at the center of gravity
v	the lateral velocity at the center of gravity
u_R	Longitudinal inflow velocity components to rudder
v_R	lateral inflow velocity components to rudder
v_m	lateral velocity at midship
w_P	Wake coefficient at propeller position in maneuvering motions
w_{P0}	Wake coefficient at propeller position in straight moving
X	Surge force around midship except for added mass

components

Y lateral force around midship except for added mass components
N_m yaw moment around midship except for added mass components
X_H Surge force around midship acting on ship hull
Y_H lateral force around midship acting on ship hull
N_H yaw moment around midship acting on ship hull
X_P Surge force due to propeller
X_R Surge force around midship by steering
Y_R lateral force around midship by steering
N_R yaw moment around midship by steering
x_G Longitudinal coordinate of the center of gravity of ship
x_H Longitudinal coordinate of the acting point of the additional lateral force component induced by steering
x_P Longitudinal coordinate of propeller position $(0.5L_{pp})$
x_R Longitudinal coordinate of rudder position $(-0.5L_{pp})$
X_w second order drift surge forces
Y_w second order drift sway forces
N_w second order drift yaw moment
α_R Effective inflow angle to rudder
β Hull drift angle at midship
β_P Geometrical inflow angle to propeller in maneuvering motions
β_R Effective inflow angle to rudder in maneuvering motions
γ_R Flow straightening coefficient
δ Rudder angle
η Ratio of propeller diameter to rudder span (D_P/H_R)
Λ Rudder aspect ratio
Ψ Ship heading angel
ρ Water density
ε Ratio of wake fraction at propeller and rudder positions $((1-w_R)/(1-w_P))$

1. INTRODUCTION

The International Maritime Organization (IMO) has implemented a technical measure (EEDI) to prevent air pollution coming from ship emissions which helps to reduce greenhouse gas (GHG) emissions coming from existing ships such as CO_2,NO_X,CH_4, and PM_{10}. These gases have been increasing the global average temperature in the world and are also harmful to the environment.

This Energy Efficiency Design Index (EEDI) measurement is mandatory for all new ships that have more than 400 Gross Tonnage (GT). The Ship Energy Efficiency for Management Plan (SEEMP) is essential for all ships. EEDI aims to reduce CO_2 emissions from ships. Consequently, In phase 4, IMO has planned to reduce it to 40% by 2030 and up to 50% by 2050. [1]

Generally, there are two EEDI calculations essential for all ships - reference or required EEDI and attained EEDI. The reference EEDI calculation is based on the reference line value parameters which is varying based on the ship type. The attained EEDI formula is based on the power of the engine, specific fuel consumption, fuel conversion factor, ship capacity, and ship speed. The attained EEDI must be smaller than the reference EEDI. This result indicates the ship emits less CO_2 and it is an energy-efficient ship.

One suggested approach to reduce CO_2 emissions is by reducing the design speed of the ship and thereby the main engine power [2]. This results in a reduced attained EEDI value which makes the ship more energy efficient and indirectly emits lesser CO_2. Due to this speed reduction, CO_2 emission will be reduced by up to 10% – 15%. However, there is a significant concern that reducing the power will leave the vessel vulnerable to course keeping in high seas and might even cause issues such as surf riding and broaching in following waves. Thus, it is important to study the effect of waves on maneuvering motions of the ship before it can be incorporated into the ship design process.

Several studies in the past and present have investigated this problem to varying level of detail [3, 4]. Evgeni Milanov et al. [4] conducted experimental study in which a scaled ship model was tested for a turning circle maneuver in a range of regular waves. The study concluded that in low speeds, the rudder effectiveness decreases significantly and it is difficult to change course. The study also concluded that short waves influence the initial turning characteristics strongly as compared to longer waves. Zhitian Xie et al.[5] developed a simulation framework that combines second order drift forces together with calm water maneuvering model to simulate the drift of vessel in waves.

This study aims to study the effect of waves on maneuvering motions by comparing the maneuvering simulations and experiments of a scaled KRISO container ship (KCS) in calm water and in regular waves. The MMG prediction method [6] is used to simulate the motion of the vessel in still water. A potential flow theory-based panel method code [7, 8] is used to calculate the second-order wave drift forces in regular waves. The standard MMG mathematical model is modified by incorporating mean wave drift forces to simulate the dynamics of ship motions in waves.

2. MMG MATHEMATICAL MODEL

The Maneuvering Modeling Group (MMG) model is used for the maneuvering prediction of the vessel in calm water and in waves which are explained in detail herein [6]. This model was proposed by the Maneuvering Modeling Group (MMG), a research group at the Japanese Towing Tank Conference (JTTC).

The non-dimensionalized 3 degree of freedom (3-DOF) maneuvering equations of motions given in [6] are modified and are given as follows:

$$(m' + m'_x)\dot{u}' - m'v'r' - x'_G m' r'^2 = X' \tag{1a}$$
$$(m' + m'_y)\dot{v}' + m'u'r' + x'_G m'\dot{r}' = Y' \tag{1b}$$
$$(I'_{zz} + x'^2_G m' + J'_{zz})\dot{r}' + x'_G m'(\dot{v}' + u'r') = N' \tag{1c}$$

In this article, prime $'$ stands for non-dimensionalized values. The forces and moment are non-dimensionalized by $(1/2)\rho L_{pp} d U_0^2$ and $(1/2)\rho L_{pp}^2 d U_0^2$ respectively. Similarly, mass and moment of inertia are non-dimentionalized by $(1/2)\rho L_{pp}^2 d$ and $(1/2)\rho L_{pp}^4 d$.Velocity and length components are non-dimentionalized by U_0 and L_{pp} respectively. Yaw rate r is non-dimentionalized as $r' = rL_{pp}/U_0$.

X', Y', and N' represent the hydrodynamic forces and moment acting on the mid-ship of the hull. These forces can be further described by components with different physical meanings, which are:

$$X' = X'_H + X'_R + X'_P + X'_W \quad (2a)$$

$$Y' = Y'_H + Y'_R + Y'_W \quad (2b)$$

$$N'_m = N'_H + N'_R + N'_P + N'_W \quad (2c)$$

According to MMG, the subscripts H, P, and R refer to the hull, propeller, and rudder. The terms corresponding to waves forces X'_W, Y'_W and N'_W are second-order drift forces which are obtained from a panel method code [7, 8]. The panel method code computes the drift forces using the near field method [9] rather than the far-field approach utilized by Maruo [3].

The coordinate system is shown in figure - 1. The axes for the earth's fixed coordinate system are $O_0 - X_0Y_0Z_0$ and the body-fixed coordinate system is $o - xyz$ where o is taken on the midship of the hull, where x, y, and z axes point toward the ship's forward, towards the starboard side, and vertically downwards respectively. The orientation of both frames is shown in Fig. 1.

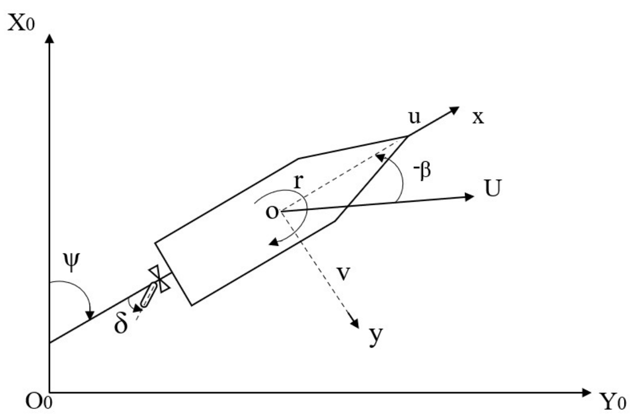

FIGURE 1: COORDINATE SYSTEM

Here, Ψ is the heading angle between the longitudinal direction of X_0 and x axis, u and v are the velocity components in the longitudinal and transverse direction of the ship respectively. Total velocity is given as $U = \sqrt{u^2 + v^2}$ and the angle between the resultant velocity and longitudinal direction of the ship is drift angle β.

2.1 Non-dimensional hydrodynamic forces and moment acting on the ship hull

X_H, Y_H and N_H are expressed using the polynomials of β and the dimensionless turning rate r', which are expressed as :

$$\beta = -\tan^{-1}\left(\frac{v}{u}\right) \quad (3a)$$

$$r' = r\left(\frac{L}{U_0}\right) \quad (3b)$$

Expressions for hydrodynamic forces and moment acting on the ship hull are obtained as follows [10]:

$$\begin{aligned} X_H + m_y v_G r_G = \left(\frac{\rho}{2} L d_{em} U_0^2\right) & \quad (4a)\\ \times \{X'_0 u'^2 + X'_{\beta\beta}\beta^2 + (X'_{\beta r} - m'_y)\beta r' + (X'_{rr} &\\ + X'_G m'_y) r'^2 + X'_{\beta\beta\beta\beta}\beta^4\} & \end{aligned}$$

$$\begin{aligned} Y_H - m_x u_G r_G = \left(\frac{\rho}{2} L d_{em} U_0^2\right) & \quad (4b)\\ \times \{Y'_\beta \beta + (Y'_r - m'_x) r' + Y'_{\beta\beta\beta}\beta^3 &\\ + Y'_{\beta\beta r}\beta^2 r' + Y'_{\beta rr}\beta r'^2 + Y'_{rrr} r'^3\} & \end{aligned}$$

$$\begin{aligned} N_H = \left(\frac{\rho}{2} L d_{em} U_0^2\right) & \quad (4c)\\ \times \{N'_\beta \beta + N'_r r' + N'_{\beta\beta\beta}\beta^3 + N'_{\beta\beta r}\beta^2 r &\\ + N'_{\beta rr}\beta r'^2 + N'_{rrr} r'^3\} & \end{aligned}$$

The hydrodynamic coefficients for the KCS vessel are taken from [10] and are reported in Table 1.

2.2 Non-dimensional hydrodynamic forces due to propeller

The propeller thrust acts only in the longitudinal direction of the ship and there is no force and moment due to the propeller in other modes of motion. Hence, the surge force due to the propeller is given as :

$$X'_P = \frac{X_P}{\frac{\rho}{2} L_{PP} d_{em} U^2} \quad (5)$$

$$X_P = (1 - t_P)T \quad (6)$$

In order to maintain simplicity, the thrust deduction factor t_P is considered to remain constant at the given propeller load. The propeller thrust T is given as

$$T = \rho n_P^2 D_P^4 K_T(J_P) \quad (7)$$

K_T is expressed as the second-order polynomial function of the propeller advanced ratio J_P which is given by

$$K_T(J_P) = K_2 J_P^2 + K_1 J_P + K_0 \quad (8)$$

where, J_p is the advance ratio and is given by

$$J_P = \frac{u(1 - w_P)}{n_P D_P} \quad (9)$$

2.3 Non-dimensional hydrodynamic forces and moment by the rudder

Rudder forces X_R, Y_R and moment N_R are expressed as:

$$X'_R = -(1 - t_R) F'_N \sin\delta \quad (10a)$$

$$Y'_R = -(1 + a_H) F'_N \cos\delta \quad (10b)$$

$$N'_R = -(x'_R + a_H x'_H) F'_N \cos\delta \quad (10c)$$

The coefficients t_R, a_H, and x'_H primarily represent the hydrodynamic interaction between the ship's hull and rudder.

TABLE 1: HYDRODYNAMIC FORCE AND MOMENT DERIVATIVES

Hydrodynamic Derivatives	Value
X_0'	-0.0167
$X_{\beta\beta}'$	-0.0544
$X_{\beta r}' - m_y'$	-0.1084
X_{rr}'	-0.0120
$X_{\beta\beta\beta\beta}'$	-0.0417
Y_β'	0.2253
$Y_r' - m_x'$	0.0398
$Y_{\beta\beta\beta}'$	1.7199
$Y_{\beta\beta r}'$	-0.4832
$Y_{\beta rr}'$	0.8341
Y_{rrr}'	-0.0050
N_β'	0.1111
N_r'	-0.0465
$N_{\beta\beta\beta}'$	0.1752
$N_{\beta\beta r}'$	-0.6168
$N_{\beta rr}'$	0.0512
N_{rrr}'	-0.0387

TABLE 2: HYDRODYNAMIC PARAMETERS FOR PROPELLER AND RUDDER

Symbols	Value
K_0	0.5228
K_1	-0.4390
K_2	-0.0609
m_x'	0.0063
m_y'	0.1552
j_{zz}'	0.0093
x_P'	-0.4565
x_R'	-0.5
x_H'	-0.436
ε	0.956
k	0.633
η	0.798
l_R'	- 0.755
t_P	0.207
w_P	0.355
t_R	0.258
a_H	0.361
$\gamma_R\ (\beta_p > 0)$	0.492
$\gamma_R\ (\beta_p < 0)$	0.338
λ	2.164
f_α	3.0058

The rudder's normal force is perpendicular to the rudder, hence, $F_N \sin\alpha$ is its component in the longitudinal direction whereas $F_N \cos\alpha$ is in the transverse direction.

Here, non-dimensionalized rudder normal force is given by

$$F_N' = \frac{A_R}{L_{pp} \cdot d} f_\alpha U_R'^2 \sin\alpha_R \tag{11}$$

where, the resultant rudder inflow velocity U_R and the angle α_R are expressed as

$$U_R' = \sqrt{u_R'^2 + v_R'^2} \tag{12}$$

$$\alpha_R = \delta - \tan^{-1}\left(\frac{v_R'}{u_R'}\right) \simeq \delta - \frac{v_R'}{u_R'} \tag{13}$$

and u_R' and v_R' are given by:

$$u_R' = \xi u'(1 - w_P)\sqrt{\eta\left\{1 + k\left(\sqrt{1 + \frac{8K_T}{\pi J_P^2}} - 1\right)\right\}^2 + (1 - \eta)} \tag{14}$$

$$v_R' = \gamma_R \cdot (v' + r' l_R) \tag{15}$$

The hydrodynamic parameters used in the simulation of motion of the KCS vessel are listed in Table 2.

3. MODEL AND EXPERIMENTAL SETUP

3.1 KCS Model

A scaled model (1 : 75.5) of the KCS vessel has been fabricated and preliminary tests were conducted for this ship model. The model is ballasted to achieve displacement and the center of gravity is determined from an inclining experiment. From the decay tests, the roll natural frequency of the model is determined as 5.236 rad/s. The main particulars of the model ship and the full-scale ship are given in Table 3.

3.2 Experimental setup

The maneuvering tests for the KCS model ship were conducted in the wave basin facility at IIT Madras. The dimensions of the wave basin are length $L = 30$ m, width $B = 30$ m and depth $d = 3.05$ m. The wave basin is equipped with a flap-type wavemaker capable of generating regular, irregular, directional, oblique, and random waves. A schematic of the wave basin is shown in Fig. 2. The maneuvering study of the KCS model ship is conducted in regular waves as shown in Fig. 3.

The experiment was performed by keeping the initial position of the model ship in head sea condition to the wave-maker as shown in Fig. 2. The vessel started from rest and was commanded to 35-degree rudder and full propeller RPM at time $t = 0$. The vessel was allowed to complete two circles in calm waters. At the completion of the second turning circle, the wave maker was activated to generate regular waves of a particular period and amplitude. Table 4 shows the experimental parameters in full scale and model scale.

The motion of the vessel is tracked using an in-house tracking system developed at IIT Madras. The angular velocities and orientations are obtained from an inertial measurement unit (IMU) mounted on board the vessel.

TABLE 3: PRINCIPLE PARTICULARS OF KRISO CONTAINER SHIP

Parameters	Model	Full-scale
Scale	1/75.5	1.00
L_{pp} (m)	3.0464	230
B (m)	0.4265	32.2
d_{em} (m)	0.143	10.8
∇ (m^3)	0.1209	52030
C_b	0.651	0.651
x_G (m)	- 0.04786	-3.614
z_G (m)	- 0.0165	-1.2468
KB (m)	0.0801	6.04746
KG (m)	0.12653	9.55317
GM (m)	0.06846	5.168428
n_p (rps)	18.15	1.925
D_P (m)	0.1046	7.9
$A_R/(L_{pp} \cdot d)$	1/54.86	1/54.86
F_n	0.26	0.26

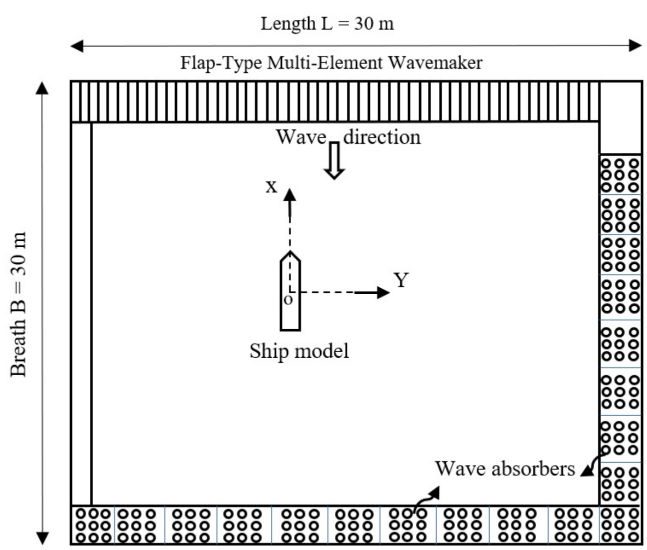

FIGURE 2: IIT MADRAS WAVE BASIN

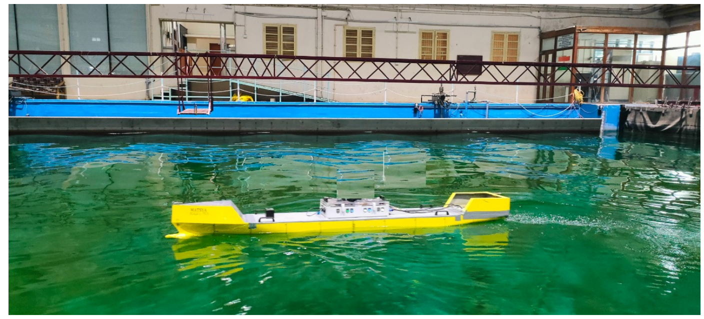

FIGURE 3: MANEUVERING OF KCS MODEL SHIP IN WAVE BASIN

TABLE 4: TEST MATRIX

Parameters	Model experiment	Full scale simulation
$v(m/s)$	1.42	12.34
$\eta(rps)$	18.5	115.5/60
$\delta(°)$	±35°	±35°
λ/L	0.513	0.513
T(sec)	1.00	8.6891
$H(m)$	0.031	2.358

4. RESULTS AND DISCUSSIONS

Fig. 4 shows the comparison of results of the turning circle maneuver in calm water. From the experiment, the turning circle diameter is $2.691L$ and for simulation, it is $2.733L$. There is a difference of 1.537% between the simulation and experiment.

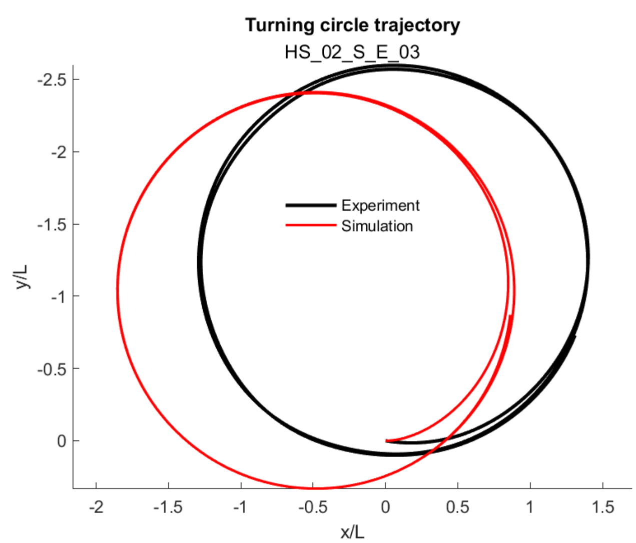

FIGURE 4: TURNING CIRCLE MANOEUVRE IN CALM WATER

It is also seen that the transient phase of the turn is significantly different between the simulation and the experiment. This can be attributed to the inherent assumption in the simulation that the hydrodynamic coefficients will be the same when the speed of the vessel is significantly less than the design speed. Also, another reason could be that the effect of propeller side wash on the wake fraction is assumed to be constant in the simulation but need not be so in the experiments [5].

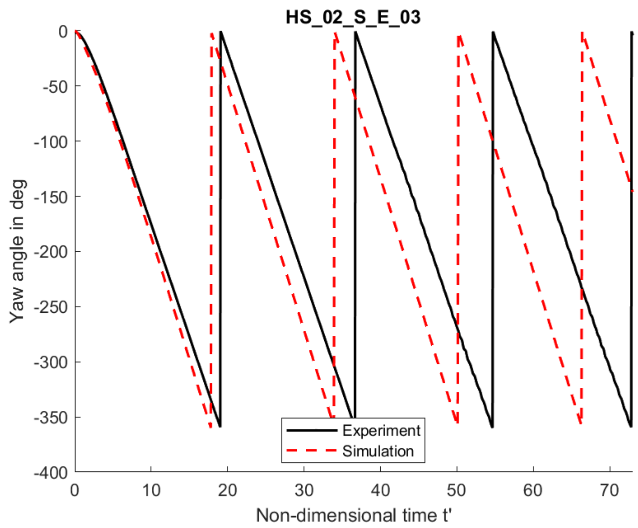

FIGURE 5: YAW ANGLE

Fig. 5 shows the plot of non-dimensionalized time vs yaw angle. This plot clearly shows that the simulation achieves the yaw angle slightly faster compared to the experiment.

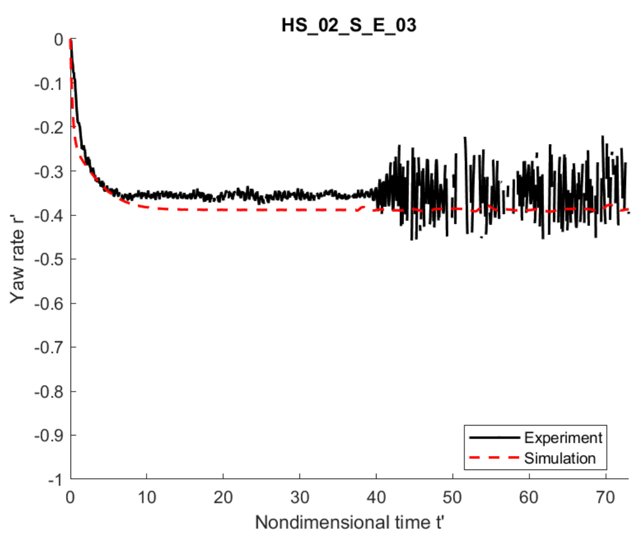

FIGURE 6: YAW RATE VS TIME

The variation in yaw rate is shown in Fig. 6. It is observed that the magnitude of the yaw rate is slightly higher in the simulation as compared to the experiment.

Fig.7 shows that both the experiment and simulation reach a steady speed at almost the same time. However, the speed achieved in the simulation is slightly higher than that achieved in the experiment. Due to this discrepancy in the achieved speed, there is a considerable difference in the trajectory obtained from

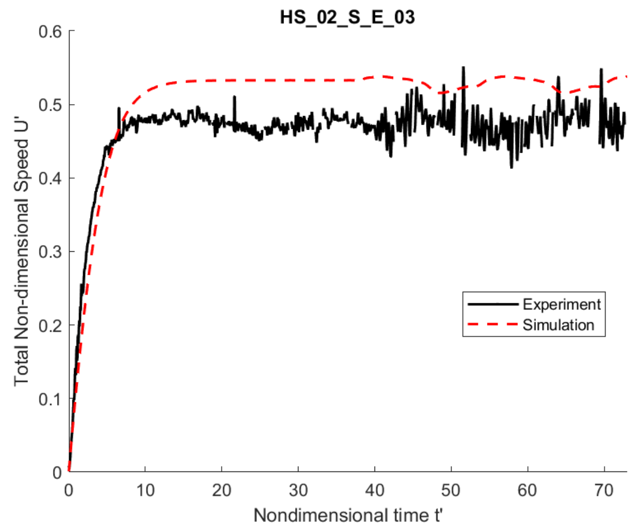

FIGURE 7: SPEED VS TIME

the experiment to that in the simulation. The model in the experiment makes a tighter turn compared to the simulation.

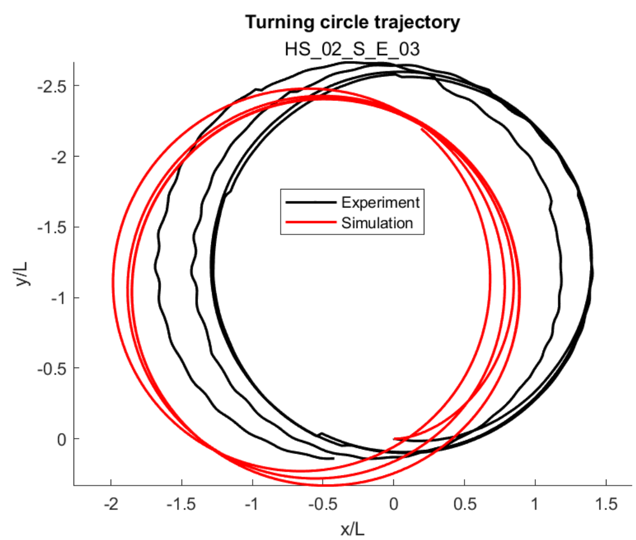

FIGURE 8: TURNING CIRCLE TRAJECTORY

A comparison of the turning circle trajectory of the vessel in experiments and simulations is shown in Fig. 8. It is observed from the experiment and numerical results that the vessel drifted along the direction of the wave. However, in simulations trajectory shows that the drift is significantly smaller compared to the experimental results.

From Fig. 9 it can be seen that the surge velocity u in the experiments is lesser compared to that in the simulation whereas the sway velocity v is more in the experiments compared to that in the simulation. This discrepancy occurs because the simulation only considers a three-degree-of-freedom model and does not consider the vessel roll dynamics. The roll motion coupled with sway and yaw motions causes a significant difference between the simulated and experimental velocities.

It is also seen that when the waves are encountered from $t' = 40$, the sway experiences considerable oscillations. From the experiment, it was also observed that the vessel experienced considerable roll motion too. In the simulation, this coupled effect between sway, roll, and yaw modes is not considered.

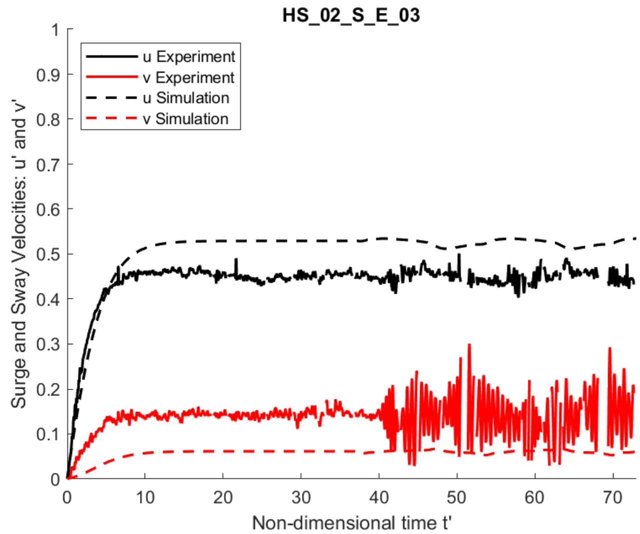

FIGURE 9: SURGE AND SWAY VELOCITIES VS TIME

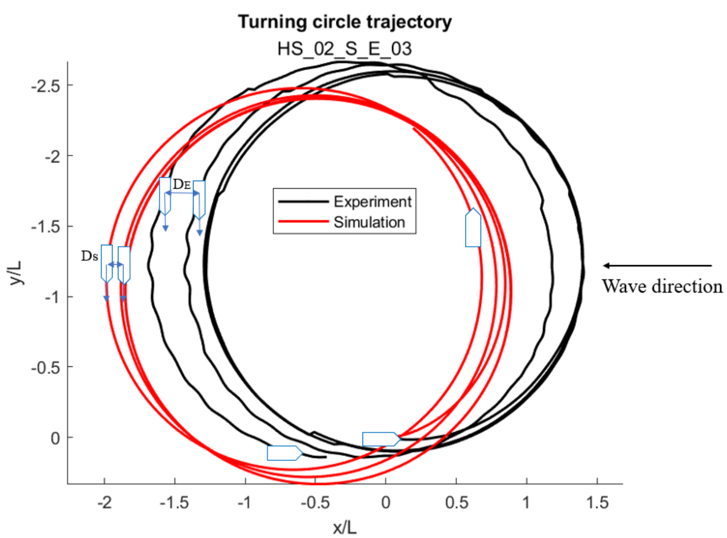

FIGURE 10: VESSEL DRIFT DISTANCE

Fig.10 shows that the vessel has drifted in the direction of the waves in both experimental and simulation trajectories. However, it is clearly seen that the experimental model ship drift distance is significantly larger than the simulation results and this can be attributed to the coupled sway and roll motion effects and the presence of first-order wave motions present in the experimental trajectory. The vessel drift distance has been calculated from the consecutive turning circles at the yaw angle of 270 degrees i.e. at the time the vessel yaw angle or longitudinal axis is exactly perpendicular to the wave direction.

The KCS vessel drift distance is considerably large in the experimental model test compared to the full-scale numerical simulation results. Especially, when the vessel turns perpendicular to the wave direction, the coupled sway and roll motion is remarkably significant. Due to this coupled effect, the vessel drift is considerably which is clearly seen from the experimental results in Fig. 10.

TABLE 5: PARAMETERS OF THE TURNING CIRCLE TRAJECTORIES IN CALM WATER AND WAVES

Test	Diameter	Yaw angle	Drift distance
Unit	m	deg	m
Experiment model	8.1978	-269.934	0.7679
Experiment Full-scale	618.93	-269.934	57.9740
Simulation model	8.3256	-269.472	0.3302
Simulation Full-scale	628.59	-269.472	24.9284

The turning circle diameter value for the model and full-scale in calm water is 2.691L and 2.733L. It has been already discussed in section 4. However, the value of the model and full-scale turning circle diameter is shown in Table 5 which is based on the length of the vessel.

The drift distance discrepancy between the experiments and simulations is 57%. The reason for this notable discrepancy is that the numerical simulations did not consider the coupled roll motion and first-order wave forces.

5. CONCLUSION

In this study, the simulation results partially match the experimental results. This discrepancy occurs because the simulation considered only a three degree of freedom model and did not include roll motion. It is observed from the experiments that a four-degree of freedom model is needed to capture the relevant dynamics. It is also important to note that the simulations consider only the second-order wave drift forces coming from the regular waves and did not include the first-order wave motions. A thorough study of maneuvering motions in different wave conditions allows us to understand the performance of the vessel in a much better way and helps improve the simulation models to better mimic the experiments.

In future studies, a four-degree-of-freedom model will be investigated that takes into account the first-order coupled wave motions along with the second-order forces so that transient roll motion and resulting coupled sway and yaw motion dynamics can be accurately captured.

6. ACKNOWLEDGMENTS

This work was partially funded by the Science and Engineering Research Board (SERB) India - SERB Grant CRG/2020/003093 and New Faculty Initiation Grant of IIT Madras. This work is also supported through the proposed Center of Excellence for Marine Autonomous Systems (CMAS), IIT Madras setup under the Institute of Eminence Scheme of Government of India.

The authors thank Professor Dr.M.Manivannan and Ms. Sai Naveena Sri MS scholar from the department of Applied Mechanics, IIT Madras who lent us their sensor to track the position of the vessel inside the wave basin. The authors would also like to thank Dr.Amitava Guha for sharing his panel method code MDLHydroD for the calculation of mean drift forces in forward speed.

REFERENCES

[1] No, Page. "Report of the Marine Environment Protection Committee on its sixty-second session." *ENVIRONMENT* Vol. 16 (2011): p. 76.

[2] TOKUŞLU, Aydın. "Analyzing the Energy Efficiency Design Index (EEDI) performance of a container ship." *International Journal of Environment and Geoinformatics* Vol. 7 No. 2 (2020): pp. 114–119.

[3] Maruo, Hajime. "The excess resistance of a ship in rough seas." *International Shipbuilding Progress* Vol. 4 No. 35 (1957): pp. 337–345.

[4] Milanov, Evgeni, Efremov, Dobrin and Anastasov, Anton. "Experimental study on KCS container ship initial turning at low speed in regular waves." *Maritime Technology and Research* Vol. 3 No. 2 (2021): pp. 102–119.

[5] Xie, Zhitian, Falzarano, Jeffrey and Wang, Hao. "A framework of numerically evaluating a maneuvering vessel in waves." *Journal of Marine Science and Engineering* Vol. 8 No. 6 (2020): p. 392.

[6] Yasukawa, Hironori and Yoshimura, Y. "Introduction of MMG standard method for ship maneuvering predictions." *Journal of Marine Science and Technology* Vol. 20 No. 1 (2015): pp. 37–52.

[7] Guha, Amitava. "Development and application of a potential flow computer program: determining first and second order wave forces at zero and forward speed in deep and intermediate water depth." Ph.D. Thesis. 2016.

[8] Guha, Amitava and Falzarano, Jeffrey. "Estimation of hydrodynamic forces and motion of ships with steady forward speed." *International Shipbuilding Progress* Vol. 62 No. 3-4 (2015): pp. 113–138.

[9] Boese, Peter. "Eine einfache methode zur berechnung der widerstandserhöhung eines schiffes im seegang." Technical report no. 1970.

[10] Yoshimura, Yasuo and Masumoto, Yumiko. "Hydrodynamic force database with medium high speed merchant ships including fishing vessels and investigation into a manoeuvring prediction method." *Journal of the Japan Society of Naval Architects and Ocean Engineers* Vol. 14 (2012): pp. 63–73.

